

# ON THE COHERENCE PROPERTIES OF FEL

Mihai Pop\*, Francesca Curbis, Sverker Werin, MAX-IV, Lund University, Lund, Sweden

## ABSTRACT

FELs are well known for generating highly coherent light with excellent brilliance. In order to improve FEL coherence we have to follow how coherence evolves along the undulator and determine the factors that influence it the most. This paper presents qualitative coherence features that shine new light on the importance of coherence studies in the design of an FEL. By simulating and then analyzing the the FEL light we arrive at results linking coherence to parameters such as undulator polarization or seed laser power density.

## METHOD

Numerical simulations have been widely used in literature [1, 2] due to their cost effectiveness and flexibility in changing any design parameter of the FEL. In our case we used the *Genesis 1.3* algorithm [3] to generate the FEL light. For extracting coherence information we devised virtual experiments that follow the physics of real experiments and applied them to the simulation results. Transverse coherence properties are studied using the Young experiment [4,5] while the longitudinal coherence is studied with Fourier analysis [6]. Although in experimental work [7] the Michelson Interferometers is used, for numerical simulations the Fourier analysis is preferred [8].

### *Spectrum and Coherence Time*

The FEL light from the simulations is generated in the form of a 4-D matrix in which one dimensions represents the position in the undulator, the following two dimensions represent the transverse coordinates (x,y) and the final dimension represents the evolution in time. As discussed in [9], the coherence time and the bandwidth are intrinsically connected, therefore once the spectrum is obtained one needs only to calculate the bandwidth and from that, the coherence time is uniquely determined.

The Spectrum at a specific point in the (x,y) plane<sup>1</sup>, at a specific position in the undulator is obtained by applying a Fourier Transform to the time evolution of the electric field intensity  $|E|^2$  and plotting it against the frequency.

### *Virtual Young's Experiment*

Transverse coherence describes the ability of two points in the transverse plane to interfere with each other. To extract transverse coherence information from our simulations we construct a mask to block all other points in the grid and rotate the mask to have the points on a horizontal line in the center of the mask. Using a 2D Fourier transform,

<sup>1</sup> We usually want to select the point which has the most intensity but one can select any other point.

we construct the interference pattern from the two points. This process is repeated for all the time slices and the interferogram is constructed by adding all the interference patterns. Having the interference pattern, we extract the visibility and multiply it with the normalized intensity to get the mutual intensity i.e., the measure of transverse coherence.

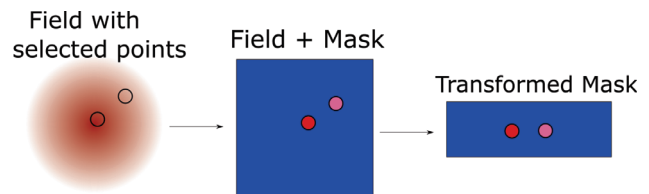


Figure 1: Representation of the process of applying a mask to the field for Young experiment.

## RESULTS AND DISCUSSIONS

The simulation input files originates from an adapted version of a generic input file from [10]. The electron nominal energy, the undulator period, the K parameter as well as the seed laser wavelength are not changed during simulations. As a guideline for our investigations we use the power output with respect to position in Figure 2 to link coherence information to the stages of FEL amplification. We infer from the plot that when seeded, the FEL saturates at 25 m and when in SASE mode the studied FEL saturates at 35 m.

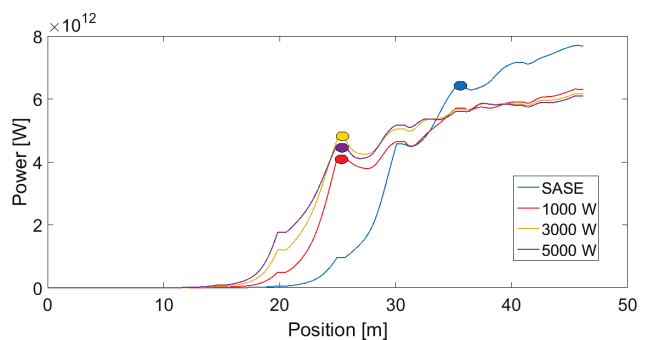


Figure 2: Power output at different positions in the undulator for different seed power, the bold points mark the beginning of saturation for each seed power.

### *Longitudinal Coherence Results*

We studied the evolution of the coherence time at different points in the undulator in a SASE FEL ( Figure 3). It can be seen that the plot has a maximum of  $\tau_{SASE} = 11$  fs at 25 m. The maximum in coherence time is achieved 10 m before power saturation (Figure 2). This means that the longitudinal coherence *saturates* earlier than the power output.

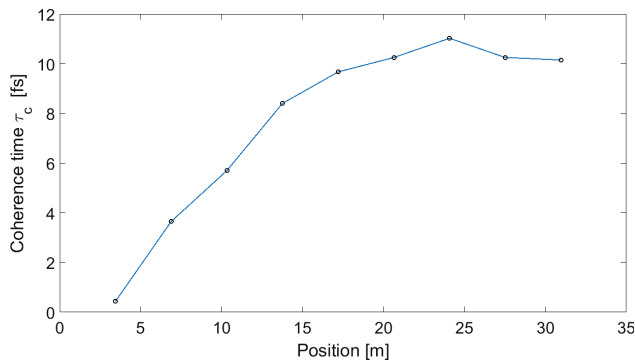


Figure 3: Coherence time  $\tau_c$  at different positions in the undulator.

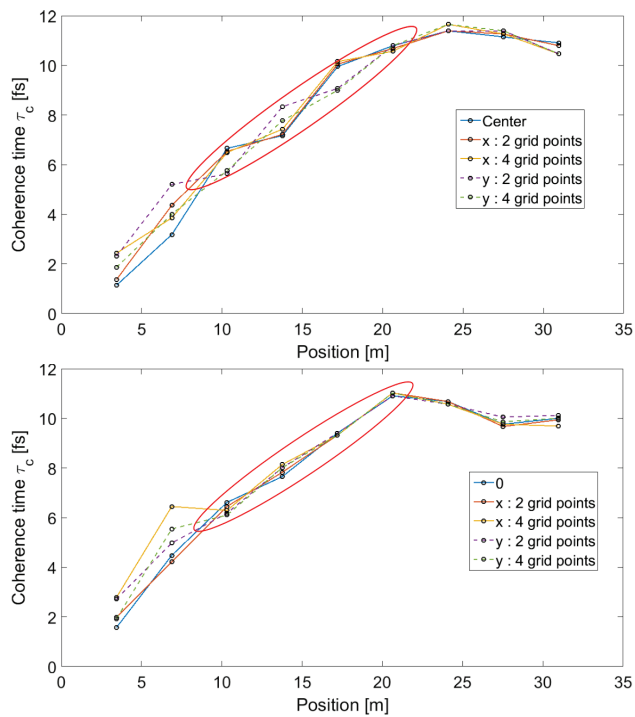


Figure 4: Coherence time  $\tau_c$  at different distances from the center of the grid in a planar undulator (top) and circular undulator (bottom).

It is important to check if the evolution of the coherence time is the same for different points in the transverse plane (Figure 4). We thus perform calculations in the center of the grid, at 2 grid points and at 4 grid points away from the center in both x and y directions. We observe only small differences between the coherence time of points located in the same plane. For the highlighted part however, coherence time at points extending in the horizontal and vertical directions are mismatched suggesting that the perturbations are coupled.

We thought of investigating this coupling feature by changing the undulator type from planar to circular because in a circularly polarized undulator the electron motion is similar in the x and y direction. Looking at Figure 4 (bottom) we see that indeed the shape of the plots is much smoother for the

highlighted part, meaning that changing from planar to circular undulator type, has eliminated the perturbation. This, however is not the only effect on temporal coherence, one can also identify that the coherence time saturates earlier in circular polarization case but that the maximum coherence time is lower than in the planar case.

### Transverse Coherence Results

The transverse correlation of the field is characterized with the Young double pin hole experiment. We use two methods when selecting the two points for the Young experiment. The selection is either symmetric or fixed point. In the symmetric selection the points selected are symmetric with respect to the center of the grid and the results give a measure of how "LASER-like" <sup>2</sup> the FEL radiation is. The fixed point selection means that the center point is kept fixed and we compare how correlated are different points with respect to the center, these calculations are an indication of how flat the wavefront and the intensity distributions are.

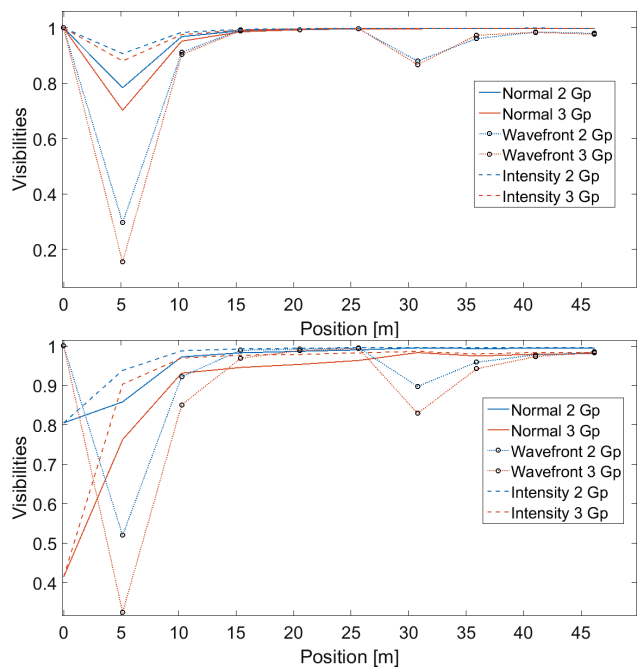


Figure 5: Transverse coherence results showing the decoupling of the angle and the intensity with respect to the total field. The two plots represent symmetric (top) and fixed center point (bottom) selection modes

We can use the fact that we are running simulations as the basis for our results and decouple the effect of the intensity and the angle on the total visibility. The results in Figure 5 are based on a seeded FEL simulation (1000 W) as to rule out the possibility of numerical noise at 0 m, where the only radiation is the seed laser in both fixed point and symmetric selection mode.

Analyzing the two plots in Figure 5 we can see that the predominant influence on the visibility of the complex field

<sup>2</sup> How well the Gaussian shape is held or how symmetric it is

is the intensity distribution. Therefore the visibility of the produced radiation is better than the seed laser visibility in fixed point calculations because the intensity of the seed laser is not as uniformly distributed as the FEL radiation. Looking at the wavefront results we notice a local minimum in the transverse coherence at the same position in the undulator where the output power reaches saturation. This detail is not present in the intensity distribution data which means that the phase information contained in the wavefront is more sensitive to detecting where saturation occurs.

Considering the previously presented result, that the FEL output radiation has a more uniform distribution of intensity than the seed laser, we now examine how does the size of the seed laser affect transverse coherence. To study this phenomenon we ran simulations in which the waist of the initial seed laser is changed by changing the Rayleigh length  $W = \sqrt{\frac{R_L \lambda}{\pi}}$  [3].

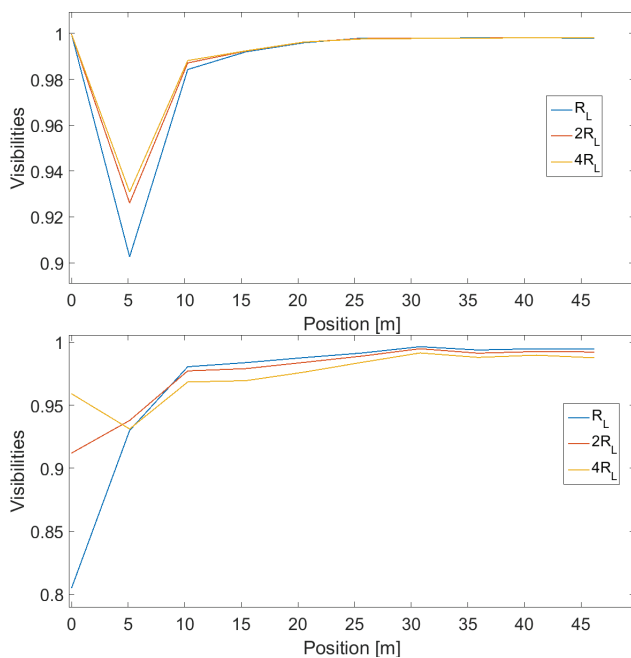


Figure 6: Visibilities from Young experiment with different Rayleigh lengths of the seed. symmetric (top), fixed center point (bottom).

An interesting feature revealed by the fixed point calculations is that even though for the smallest  $R_L$  the visibility starts off worse, it actually reaches higher values than the other ones. This leads us to believe that the uniformity of the intensity distribution in an FEL is dependent on the power density which initiates the FEL process, not on the homogeneity of the Seed laser. This being said, we see little influence on the maximum transverse coherence by changing the waist of the seed laser.

## CONCLUSIONS

Using existing FEL simulation codes and our own developed analysis tools we have shown that the undulator type has a large influence on the evolution of the longitudinal coherence in a SASE FEL. Furthermore Virtual Young’s experiment results revealed that the power density of the seed laser and not the total power is the key factor in how transversely coherent the FEL light is. Lastly we decoupled the intensity from the wavefront information and showed that transverse coherence is more sensitive to the intensity distribution than to the wavefront shape.

## REFERENCES

- [1] Chubar Oleg et al. Time-dependent fel wavefront propagation calculations: Fourier optics approach. *Nuclear Instruments and Methods in Physics Research Section A: Accelerators, Spectrometers, Detectors and Associated Equipment*, 593(1):30–34, 2008.
- [2] E. L. Saldin, E. A. Schneidmiller, and M. V. Yurkov. Self-amplified spontaneous emission fel with energy-chirped electron beam and its application for generation of attosecond x-ray pulses. *Phys. Rev. ST Accel. Beams*, 9:050702, May 2006.
- [3] Sven Reiche. *Genesis 1.3 User Manual*.
- [4] Ivan A. Vartanyants and Andrej Singer. *Coherence Properties of Third-Generation Synchrotron Sources and Free-Electron Lasers*, pages 821–863. Springer International Publishing, Cham, 2016.
- [5] Inoue Ichiro et al. Characterizing transverse coherence of an ultra-intense focused x-ray free-electron laser by an extended young’s experiment. *IUCrJ*, 2(6), 2015.
- [6] Lutful Ahad et al. On spectral and temporal coherence of x-ray free-electron laser beams. *Optics Express*, 24(12):13081–13090, 2016.
- [7] S. Roling et al. Time-dependent wave front propagation simulation of a hard x-ray split-and-delay unit: Towards a measurement of the temporal coherence properties of x-ray free electron lasers. *Phys. Rev. ST Accel. Beams*, 17:110705, Nov 2014.
- [8] E.L. Saldin, E.A. Schneidmiller, and M.V. Yurkov. Coherence properties of the radiation from x-ray free electron laser. *Optics Communications*, 281(5):1179 – 1188, 2008.
- [9] Joseph W. Goodman. *Statistical Optics*. Wiley, 2000.
- [10] Sven Reiche. <http://genesis.web.psi.ch/inputfiles.html> ttf fel, June 2016.